DOI: 10.36108/laujoces/6202.61.0262

Finite Element Analysis of the Thermo-Mechanical Behaviour of Rigid Pavement under Seasonal Temperature Variations Using Abaqus.

*[1]Oyaotuderekumor, O. I. and [2]Akintude, O.P

[1,2]Department of Civil Engineering, University of Ibadan, Ibadan, Oyo State, Nigeria.

*Corresponding Author E-mail: aoadebayo96@gmail.com Tel: 08139155449

Abstract

The study adopted a sequential methodology beginning with the collection of meteorological records, pavement geometric characteristics, and traffic loading data to establish realistic boundary and loading conditions. Additionally, temperature-dependent thermal and mechanical properties of concrete were experimentally evaluated in accordance with relevant ASTM and BS standards. Subsequently, a three-dimensional finite element model was developed in ABAQUS to simulate combined thermal cycles and wheel loading effects. The resulting deflection, stress, and strain responses were statistically analysed using SPSS to examine their variation and interrelationships across different temperature regimes. Meteorological analysis indicated mean annual ambient temperatures of 35.5 °C, 36.7 °C, 34.7 °C, and 38.5 °C for 2024, 2023, 2022, and 2021, respectively. The pavement structure consisted of a jointed plain concrete pavement with a slab thickness of 240 mm, slab width of 3.75 m, and transverse joint spacing of 3.5 m. Furthermore, axle load analysis produced equivalent standard axle factors of 0.56, 1.50, 2.25, and 3.00 for light vans, medium trucks, cement trucks, and fuel tankers, respectively. Experimental results showed a consistent decline in thermal conductivity, specific heat, flexural strength, and elastic modulus with increasing temperature. Correspondingly, numerical simulations revealed progressive increases in pavement deflection, strain, and stress between 25 °C and 40 °C. Correlation analysis further demonstrated near-perfect relationships among these responses, with coefficients exceeding 0.97, indicating highly predictable thermo-mechanical behaviour. Overall, the findings confirm that elevated temperatures significantly degrade concrete performance; therefore, the incorporation of supplementary cementitious materials is recommended to improve thermal stability and ensure long-term pavement durability.

Keywords: Rigid Pavement, Thermo-Mechanical Behaviour, Finite Element Modelling, ABAQUS, Thermal Gradients, Deflection, Stress–Strain Response.

Introduction

Pavement systems are fundamental to modern transportation infrastructure, serving as the structural platform that ensures safe, efficient, and sustainable vehicular movement across diverse climatic zones. Their performance and durability are significantly influenced by external environmental conditions in addition to mechanical stresses from repeated traffic loading. Among these environmental factors, seasonal temperature variations exert a profound influence on the structural behaviour of pavements, altering their mechanical and thermal properties over time. Such fluctuations often lead to issues like cracking, warping, and differential stress development, which in turn compromise service life and increase maintenance costs (Yannis and Chaziris, 2022; Al-Atroush, 2022). Consequently, a detailed understanding of the thermo-mechanical responses of pavements is indispensable for developing climate-resilient infrastructure that can adapt to changing environmental conditions.

Furthermore, the two major categories of pavement systems—flexible and rigid—exhibit different behavioural patterns when exposed to temperature variations. Flexible pavements, which are predominantly asphalt-based, are viscoelastic and highly sensitive to temperature fluctuations. Elevated temperatures reduce asphalt stiffness, thereby increasing susceptibility to rutting, while low temperatures induce brittleness, resulting in thermal cracking (Ma *et al.,* 2024). In contrast, rigid pavements, usually constructed from Portland cement concrete, possess comparatively elastic properties but remain vulnerable to thermal gradients that generate curling and warping stresses across slab thickness. These stresses are particularly problematic in regions where temperature cycles are pronounced, leading to premature distresses that accelerate deterioration (Al-Qadi and Hernandez, 2021). Thus, understanding how rigid pavements respond to seasonal temperature variations is central to improving their design and performance.

In recent decades, the Finite Element Method (FEM) has emerged as a critical analytical tool for predicting pavement behaviour under coupled thermal and mechanical conditions. FEM provides an advanced framework for capturing complex material responses, stress distributions, and failure mechanisms with a degree of precision that traditional empirical methods cannot achieve. Among the software platforms that implement FEM, ABAQUS has distinguished itself with robust thermo-mechanical coupling capabilities, advanced contact algorithms, and the ability to model nonlinearities associated with temperature-dependent material properties (Liu *et al.,* 2022; Benchekkour *et al.,* 2024). Despite these advantages, the systematic application of ABAQUS in evaluating the thermo-mechanical behaviour of rigid pavements under seasonal temperature variations remains limited, as much of the existing body of research has either focused on flexible pavements or considered isolated performance indicators.

Consequently, there is a pressing need to bridge this gap by integrating experimental, climatic, and modelling approaches to simulate the actual behaviour of rigid pavements under realistic seasonal cycles. Empirical pavement design methodologies, while widely used, often fail to capture the nonlinear and time-dependent interactions between environmental loads and material responses, thereby limiting their reliability in predicting long-term performance (Qin *et al.,* 2022). By contrast, performance-based and mechanistic-empirical approaches, underpinned by finite element modelling, offer more reliable predictions for pavement resilience in the face of climate variability. This study, therefore, seeks to contribute to this evolving discourse by applying ABAQUS to comprehensively analyse the thermo-mechanical behaviour of rigid pavements under seasonal temperature variations, providing insights that are both theoretically grounded and practically relevant.

Despite substantial progress in pavement engineering research, a persistent problem remains: rigid pavements are continuously exposed to traffic-induced stresses in addition to the pronounced effects of seasonal temperature fluctuations. These variations induce thermal gradients across pavement slabs, leading to curling, warping, and thermally induced cracking, all of which accelerate structural deterioration (Llopis-Castelló *et al.*, 2020; Wu and Mahdi, 2022). Yet, design methodologies in many regions still rely heavily on empirical principles that inadequately address the coupling of thermal and mechanical influences. The lack of systematic studies that employ advanced finite element tools such as ABAQUS to investigate these coupled behaviours in rigid pavements underscores a critical knowledge gap, which, if unaddressed, will continue to undermine the reliability of pavement design frameworks.

The significance of this study lies in its potential to strengthen the reliability and precision of pavement performance predictions under combined thermal and mechanical influences. As climate variability intensifies, the durability of rigid pavements is increasingly at risk, making it vital to understand how these structures behave under prolonged cycles of expansion and contraction. Through the advanced modelling capabilities of ABAQUS, this study offers practical insights into the deformation mechanisms, stress development, and failure risks of rigid pavements under seasonal temperature variations. These insights will provide engineers, designers, and policymakers with evidence-based guidance for adopting performance-oriented pavement design, selecting materials with improved thermal compatibility, and optimising slab dimensions to enhance service life and reduce maintenance costs (Wu and Mahdi, 2022; Benchekkour *et al.*, 2024).

Research Methodology

This study adopted a systematic methodological framework to investigate the thermo-mechanical behaviour of rigid pavements under seasonal temperature variations using the finite element method (FEM) in ABAQUS. The procedures were organised into sequential stages covering data collection, thermo-mechanical characterization of materials, finite element modelling, and statistical data analysis.

Data Collection

This objective commenced with a site-specific investigation to gather meteorological data, such as ambient temperature fluctuations, solar radiation, and rainfall, from the Nigerian Meteorological Agency. Pavement geometry, including layer thicknesses, slab dimensions, and joint spacing, was obtained from local road authorities or through field surveys. Traffic loading data (axle configurations and load spectra) and boundary conditions (support conditions and interface behaviour) were defined in accordance with AASHTO or Nigerian highway design guidelines. The information served as input parameters for the FEM simulation. Concrete samples were prepared to replicate the geometry and material properties of the pavement section under study.

Thermo-Mechanical Characterization

Laboratory testing was performed to determine the thermal and mechanical properties of the pavement concrete. The thermal conductivity and specific heat capacity were measured using a Hot Disk Thermal Constants Analyzer (TPS 2500 S, Hot Disk AB, Sweden, accuracy ±5%). The coefficient of thermal expansion was obtained using a Netzsch Dilatometer (Model DIL 402 Expedis Supreme, Germany, measurement range −180 °C to 1550 °C, accuracy ±0.1%). Mechanical properties including elastic modulus and flexural strength were evaluated using a Universal Testing Machine (Instron 5982, USA, capacity 100 kN, precision ±0.5%) at temperature ranges of 25 °C, 30 °C, 35 °C, and 40 °C. All tests were conducted in accordance with ASTM C469 (elastic modulus), ASTM C78 (flexural strength), and ASTM E228 (thermal expansion).

Finite Element Modelling

A three-dimensional finite element model of jointed rigid pavement was developed in ABAQUS/CAE (Dassault Systèmes, France, Version 2022). The model incorporated the pavement slab, base layer, and supporting subgrade. The slab geometry followed dimensions obtained from the field, while the material properties were defined based on laboratory results. Contact and boundary conditions were specified to replicate realistic field conditions, with interface friction modelled using a coefficient of 0.6. Seasonal temperature variations were introduced as time-dependent thermal loads to simulate annual variations across wet and dry seasons. Traffic loads were represented as both static and moving wheel loads applied through surface pressure distributions. Outputs monitored included stress fields, displacement contours and strain distributions, providing a holistic evaluation of pavement responses under coupled thermal and mechanical effects.

Data Analysis

The simulation outputs were exported to IBM SPSS Statistics (Version 27, IBM Corp., USA) for statistical processing. The primary performance metrics analysed were vertical deflections, tensile stresses, and strain responses across the temperature ranges of 25 °C, 30 °C, 35 °C, and 40 °C. Data were organised into observation-based datasets for comparative analysis. Pearson correlation analysis was applied to evaluate the relationships among deflection, stress, and strain, providing insights into interdependencies of thermo-mechanical responses. The significance of differences across temperature conditions was determined using one-way ANOVA at a 95% confidence level ($p < 0.05$).

Results and Discussion

Finite Element Modelling Parameters

Meteorological Data

The meteorological dataset from 2010 to 2024 presents an important basis for evaluating the thermo-mechanical performance of rigid pavements under seasonal temperature variations. The recorded ambient temperatures fluctuated between 31.4 °C and 39.5 °C, with 2015 exhibiting the highest mean value at 39.5 °C while 2017 and 2011 recorded lower values at 31.4 °C. These fluctuations highlight the significant thermal cycles that pavement structures are subjected to, which in turn influence curling, warping, and thermal stress development within the slab. Sub-ambient temperatures, ranging from 20.9 °C to 23.6 °C, reveal a relatively stable lower-bound condition but still indicate seasonal cooling effects that could intensify tensile stresses at the slab bottom. These findings align with the work of Qiao *et al.*, (2020), who emphasized that regional temperature fluctuations serve as critical determinants in the long-term durability of concrete pavements, particularly in climates with high diurnal and annual variability.

Precipitation values show an inconsistent distribution, with the highest value at 131.1 cm in 2019 and the lowest at 105.2 cm in 2015. Such variations play a critical role in the moisture regime of the pavement foundation layers, thereby influencing stiffness and the overall load distribution. Meanwhile, solar radiation exhibited significant variation, ranging from 193.18 W/m² in 2016 to 276.43 W/m² in 2021 as illustrated in Table 1. This parameter is particularly relevant, as increased solar radiation intensifies surface heating, creating non-uniform temperature gradients across pavement depth.

Table 1: Annual Meteorological Data from 2010 –2024.

Year	Ambient Temperature (°C)	Sub-ambient temperature (°C)	Precipitation (cm)	Mean Solar Radiation (W/m²)
2024	35.5	21.8	130.7	235
2023	36.7	22.8	126.7	241.87
2022	34.7	21.2	124.2	260.72
2021	38.5	23.6	113.1	276.43
2020	34.3	21.8	126.8	243.44
2019	32.2	21.7	131.1	241.87

2018	33.3	22.9	127.7	223.03
2017	31.4	21.7	117.2	194.75
2016	35.7	20.9	121.5	193.18
2015	39.5	21.5	105.2	201.47
2014	33.5	21.8	116.1	224.62
2013	38.9	21.5	108.8	254.44
2012	33.2	22.6	125.6	267.49
2011	31.4	21.5	107.2	231.34
2010	34.9	22.3	125.8	240.17

Source: *Nigerian Meteorological Agency (Nimet).*

Pavement Geometry and Structural Configuration

The modelled pavement represents a Jointed Unreinforced Concrete Pavement (JUCP), which is one of the most commonly adopted configurations for high-traffic highways. The geometry incorporates a slab thickness of 240 mm, a width of 3.75 m, and joint spacings of approximately 3.5–3.63 m in both transverse and longitudinal directions as shown in Table 2. The significance of these dimensions lies in their influence on structural load transfer, curling response, and thermal restraint. Thicker slabs generally provide enhanced load-bearing capacity but simultaneously generate higher thermal stresses due to restricted flexibility. This relationship has been emphasized by Yang *et al.*, (2018), who reported that slab thickness strongly correlates with thermal cracking susceptibility in regions of elevated temperature gradients.

The transverse and longitudinal joint spacing are nearly equal, indicating a uniform joint pattern designed to minimize slab restraint and dissipate thermal strains effectively. The short spacing is 3.5 – 3.63 m is consistent with standards for rigid pavements in regions prone to thermal warping. According to Ceylan *et al.*, (2016), reduced joint spacing mitigates the risk of mid-slab cracking by lowering the magnitude of thermally induced curling stresses. However, it also increases the number of joints, which can introduce durability concerns related to faulting and spalling. The JUCP type, unlike continuously reinforced concrete pavements (CRCP), relies heavily on joint efficiency and load transfer devices rather than distributed reinforcement. This choice is appropriate for developing economies where construction simplicity and cost efficiency are prioritized. Nevertheless, such configurations require precise modelling of joint behaviour in finite element analysis, as joints remain the weakest structural locations under thermal and traffic loads.

Table 2: Geometric and Structural Characteristics of the Modelled JUCP Pavement

Pavement type	Jointed Unreinforced Concrete Pavement (JUCP)
Traffic level	High (highways)
Slab thickness (mm)	240
slab width (m)	3.75
Transverse joint spacing (m)	3.5
Longitudinal joint spacing (m)	3.63

Loading and Boundary Conditions

The axle configurations and load data provide critical insight into the mechanical demands placed on the pavement structure. The results indicate the presence of multiple truck classes, ranging from small delivery vans with single axles (45 kN, 0.56 E80) to heavy quad-axle fuel tankers with loads as high as 240 kN and equivalency factors up to 3.0. This variation illustrates the diverse load spectrum that the pavement is subjected to, reflecting realistic highway traffic conditions. Equivalent single axle load (ESAL) factors show a progressive increase with higher axle configurations, highlighting the nonlinear relationship between axle grouping and pavement damage.

The axle load frequency distribution further demonstrates that 37.5% of observed loads fall within the 61–100 kN range, with an additional 30% between 101–150 kN. This suggests that medium to heavy trucks dominate traffic conditions, which substantially accelerates pavement deterioration compared to lighter loads. Although only 2.5% of axles exceed 200 kN, their impact on pavement life remains disproportionately high due to the fourth-power relationship between axle load and structural damage as presented in Table 3 and 4. In line with this, Moffatt, (2015), reported that infrequent but extreme axle loads often govern rigid pavement performance and service life, requiring detailed representation in structural modelling.

Table 3: Axle Configurations, Loadings, and Equivalent Standard Axle Factors (E80)

Truck Type	Axle Configuration	Axle Load (kN) (Awosanya *et al.*, 2023)	Standard Axle Equivalent (E80) (Federal Republic of Nigeria, Federal Ministry of Works, 2013)
Small Delivery Van	Single	45	0.56
Medium Truck	Tandem	120	1.5
Heavy Cement Truck	Tridem	180	2.25
Fuel Tanker	Quad	240	3

Table 4: Axle Loads and Percentage Frequencies.

Days	Single Axle Loads	Tandem Axle Loads	Tridem Axle Loads	Quad Axle Loads
Monday	13	28	28	12
Tuesday	21	32	17	8
Wednesday	19	30	25	7
Thursday	12	28	29	9
Friday	16	32	21	14
Total	80	150	120	50
Average	16	30	24	10
Percentage (%)	20%	37.5%	30%	12.5%

Thermo-Mechanical Characterization

Thermal Properties of Concrete

The results presented in Table 5 illustrate that the thermal conductivity of concrete decreased progressively with rising temperature, falling from 2.17 W/m·K at 25 °C to 1.84 W/m·K at 40 °C. This reduction signifies that the ability of the concrete to transfer heat declined as the internal microstructure became more porous and less compact under thermal expansion. Similarly, the specific heat capacity also exhibited a consistent decline from 0.90 kJ/kg·K to 0.77 kJ/kg·K across the same temperature range. This indicates that the concrete's capacity to absorb and store thermal energy reduces at elevated temperatures, making it more susceptible to rapid thermal fluctuations. Such trends are consistent with findings that attribute the thermal degradation of cementitious composites to the evaporation of bound water and changes in pore connectivity (Wu *et al.,* 2018). Consequently, the thermal environment directly affects how rigid pavements dissipate and accumulate heat, which in turn influences their overall durability.

Moreover, at moderate temperatures such as 30 °C, the decrease in both conductivity (2.05 W/m·K) and specific heat (0.85 kJ/kg·K) already signals the onset of thermo-physical instability. This behavior suggests that seasonal variations in tropical and sub-tropical regions may accelerate deterioration due to higher temperature cycles. When the material becomes less effective at transferring and buffering heat, significant thermal gradients can develop across the pavement depth, inducing curling and warping stresses. A similar observation was reported in a recent study where high surface temperatures caused greater thermal gradients between the top and bottom of concrete slabs, leading to increased incidences of corner cracks (Safiuddin *et al.*, 2018).

Furthermore, at extreme conditions, particularly at 40 °C, the reduction in thermal conductivity to 1.84 W/m·K and specific heat to 0.77 kJ/kg·K becomes critical as illustratedin Table 4.4. This implies that the concrete is not only retaining heat longer at the surface but is also unable to distribute it evenly through its depth, thereby intensifying internal stress concentrations. In practical terms, this exacerbates the risk of thermal fatigue, where repeated heating and cooling cycles weaken the pavement matrix over time. Similar conclusions were drawn in a computational analysis where thermal resistance at high temperatures was linked to microcracking and decreased structural resilience (Gong *et al.,* 2023). Hence, the observed thermal degradation highlights the importance of considering climate-specific boundary conditions during design, particularly in regions where pavement exposure to prolonged high temperatures is inevitable.

Table 5: Effect of Temperature on Thermal Properties of Concrete

Temperature (°C)	Thermal Conductivity (W/m·K)	Specific Heat (kJ/kg·K)
25	2.17	0.9
30	2.05	0.85
35	1.91	0.8
40	1.84	0.77

Mechanical Properties of Concrete

The mechanical performance of concrete with temperature rise, particularly in terms of flexural strength and elastic modulus in Table 6 reveals a significant reduction. At 25 °C, the flexural strength was 4.96 MPa and the elastic modulus was 37.6 GPa, values consistent with conventional ranges for pavement-grade concrete. However, as the temperature increased to 30 °C, both parameters showed notable reductions: flexural strength dropped to 4.15 MPa, while elastic modulus fell to 31.5 GPa. This deterioration demonstrates the sensitivity of concrete's load-carrying and deformation resistance to elevated temperatures. Such reductions can be explained by the softening of the cement matrix and the weakening of interfacial transition zones, leading to

microstructural instability. Previous experimental work corroborated this behavior, reporting that concrete subjected to elevated temperatures exhibited declining stiffness due to the breakdown of hydration products and increased micro cracking (Smarzewski, 2019).
Similarly, at higher thermal regimes of 35 °C, the flexural strength declined further to 3.27 MPa and the modulus dropped sharply to 24.8 GPa. This reduction is particularly significant because flexural resistance governs the ability of pavements to withstand tensile stresses induced by traffic and environmental gradients. A similar outcome was reported in a numerical study where reduced stiffness at elevated temperatures was shown to amplify stress magnitudes under both thermal and mechanical loads, leading to premature slab failure (Kildashti *et al.,* 2024). The most critical observation occurs at 40 °C, where flexural strength fell to 3.11 MPa and the elastic modulus to 23.5 GPa. Such low stiffness and tensile resistance levels indicate that the material enters a vulnerable state where even moderate traffic loading could precipitate cracking or corner break failures.

Table 6: Variation of Flexural Strength and Elastic Modulus of Concrete with Temperature

Temperature (°C)	Flexural Strength (MPa)	Elastic Modulus (GPa)
25	4.96	37.6
30	4.15	31.5
35	3.27	24.8
40	3.11	23.5

Rigid Pavement Modelling

The results displayed in Figure 1–4 demonstrate a clear and progressive increase in deflection values as the temperature rises from 25°C to 40°C. This steady growth across all observations highlights the direct influence of thermal loading on rigid pavement behaviour. At 25°C, deflections begin at lower magnitudes but consistently increase with each temperature increment, reaching their highest values at 40°C. This pattern reflects the cumulative nature of thermal expansion within the pavement structure, where the rising temperature induces additional stresses and deformations. Similar findings were reported by Subedi *et al.* (2025), who emphasized that rigid pavements exhibit linear increases in displacement when subjected to uniform thermal gradients, largely due to the expansion of cementitious materials.

Higher deflection magnitudes are observed in the first four observations, with values rising from 0.557 mm at 25°C to 0.731 mm at 40°C. These results suggest that certain zones of the pavement are more susceptible to temperature-induced displacement, possibly due to stress concentration or material heterogeneity. The smooth and continuous increase in these observations indicates a uniform slab response under heating. This agrees with the study of Pour (2023), who found that rigid pavements subjected to higher surface temperatures display consistent slab lifting and bending, particularly at critical load transfer areas.

In the mid-range observations, such as those between 0.3189 mm and 0.5307 mm, the deflection values reveal a sharper rise after the initial temperature, particularly beyond 30°C. This indicates that thermal effects may reach a threshold, where expansion accelerates due to the combined influence of temperature rise and structural constraints. The observed nonlinearity in these ranges corresponds to the work of Li *et al.* (2024), who reported that pavement slabs experience more rapid deformation growth beyond certain temperature limits, especially when support conditions are weak or differential gradients are present.

The lower deflections recorded in the last group of observations, ranging from 0.0514 mm at 25°C to 0.1841 mm at 40°C, show that even the least responsive areas of the pavement are still affected by thermal variation. Although the magnitudes remain small, the consistent upward trend signifies that no portion of the pavement is entirely exempt from thermal loading effects. This aligns with the study of Al-Atroush. (2022), who observed that rigid pavements, regardless of initial deflection levels, undergo progressive thermal-induced movements, with critical implications for long-term durability.

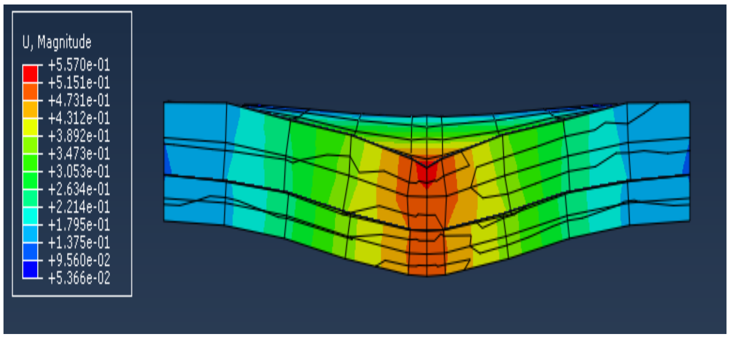

Figure 1: Deflection Magnitude of the Structural Model at 25 °C

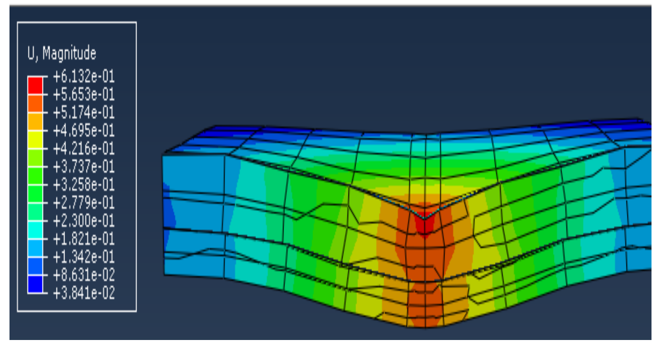

Figure 2: Deflection Magnitude of the Structural Model at 30 °C

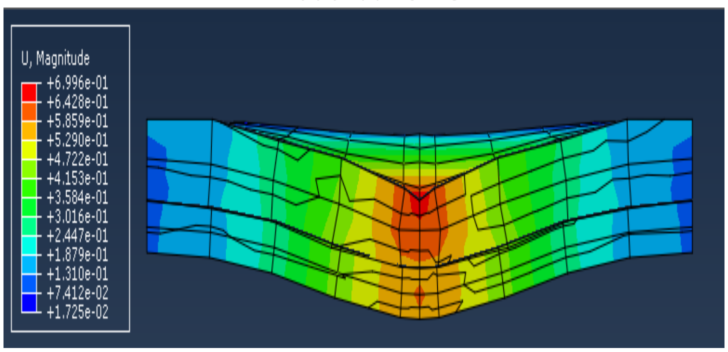

Figure 3: Deflection Magnitude of the Structural Model at 35 °C

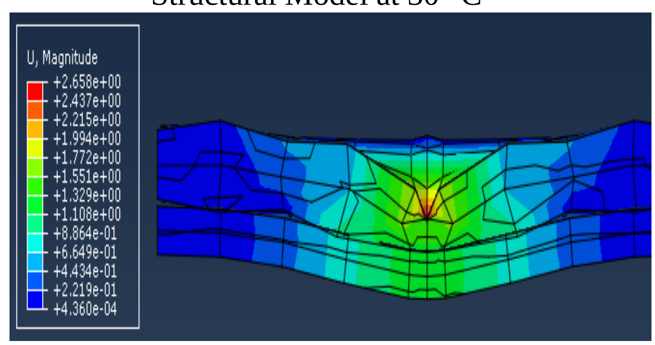

Figure 4: Deflection Magnitude of the Structural Model at 40 °C

The results presented in Figure 5–8 reveal how stress magnitudes within the rigid pavement model respond to changes in temperature from 25°C to 40°C. A general upward trend is observed across most observations, with stress values progressively increasing as the temperature rises. The first four observations show the highest stress magnitudes, rising sharply from 3280 N/m² at 25°C to 3951 N/m² at 40°C. This continuous growth pattern indicates that pavement slabs are more vulnerable to stress concentration at higher temperatures, a finding consistent with the report of Alsheyab et al. (2024), who noted that thermal gradients magnify internal stresses within concrete pavements, leading to higher risks of fatigue failure.

For the middle group of observations, a steady increase in stress is also evident, though with some fluctuations at intermediate temperatures. For instance, observation 5 experiences a dip at 30°C before rising again to 2871 N/m² at 40°C, while observations 6 and 7 show slight reductions between 25°C and 30°C, followed by consistent recovery. These minor variations suggest that the pavement's structural response may not always be linear, as local conditions such as material heterogeneity and restraint from subgrade support can temporarily reduce stress magnitudes before thermal expansion dominates. Similar non-linear patterns were described by Al-Khateeb et al.

(2025), who found that rigid pavements exhibit irregular stress fluctuations at mid-range temperatures due to uneven distribution of thermal loads across the slab.

In the lower observation set, particularly from observations 10 to 13, the stress magnitudes begin from relatively low values but exhibit notable dips at 30°C before recovering at higher temperatures. For example, observation 12 decreases significantly from 597 N/m² at 25°C to 485 N/m² at 30°C, before rising to 729 N/m² at 40°C. Likewise, observation 13 records the lowest stress levels overall, dropping sharply at 30°C and then gradually recovering. These fluctuations at the lower end indicate that stress distribution in pavement slabs may not be uniform across all regions, with weaker or less restrained zones responding differently to thermal expansion. This behaviour corresponds with findings by Li et al. (2025), who observed that stress distribution within concrete slabs is spatially variable and more sensitive to localised temperature gradients in thinner or less stiff sections.

Overall, the stress distribution results show that thermal loading has a strong influence on pavement behaviour, with most regions experiencing progressive stress increases as temperatures rise. However, the presence of dips at 30°C in several observations highlights the complexity of thermo-mechanical interactions, where local variations in material and support conditions can temporarily offset stress build-up. These results reinforce the importance of finite element modelling in capturing such nuanced behaviours and align with recent studies demonstrating that rigid pavements are highly sensitive to temperature-induced stress variations, particularly under seasonal cycles (Bayraktarova *et al.*, 2022).

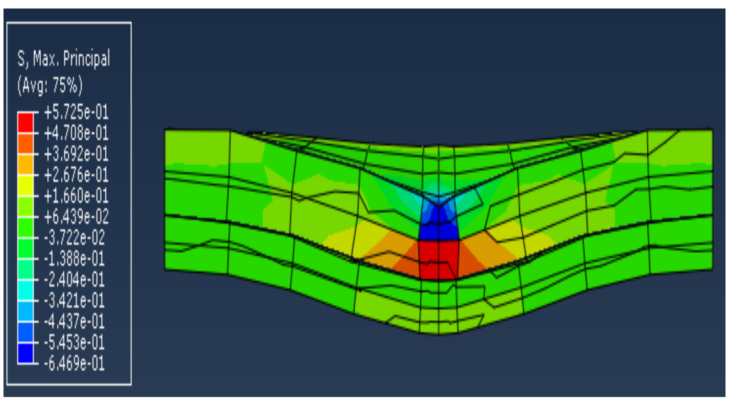

Figure 5: Stress Distribution Magnitude of the Structural Model at 25 °C

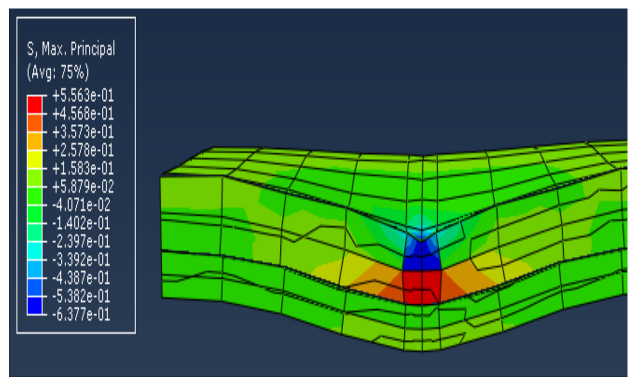

Figure 6: Stress Distribution Magnitude of the Structural Model at 30 °C

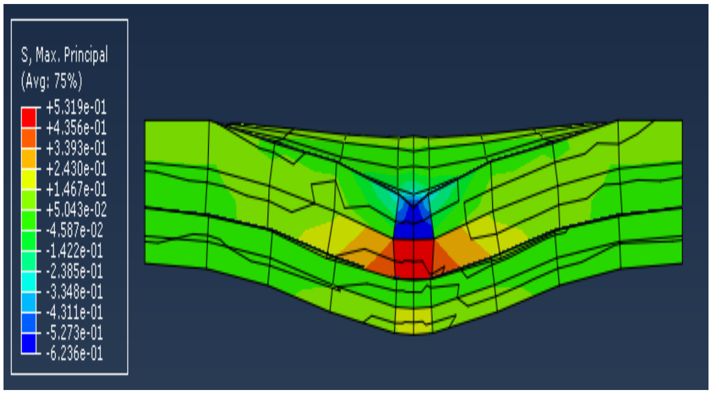

Figure 7: Stress Distribution Magnitude of the Structural Model at 35 °C

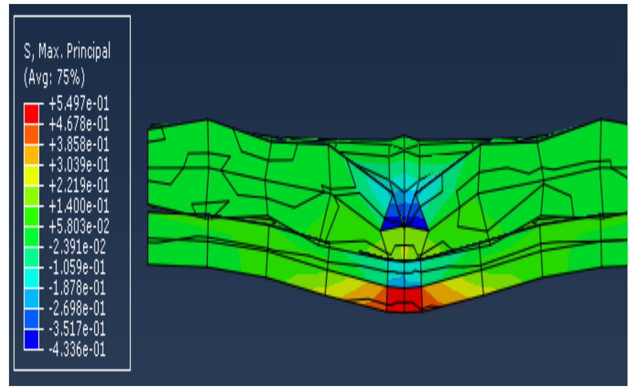

Figure 8: Stress Distribution Magnitude of the Structural Model at 40 °C

The results presented in Figure 9–12 show the variation of strain magnitudes within the rigid pavement model across different temperature conditions from 25°C to 40°C. A uniform upward trend is evident across all observations, with strain consistently increasing as temperature rises. The highest values are recorded in the first observations, where strain grows from 0.00411 at 25°C to 0.00532 at 40°C. This steady progression demonstrates that thermal expansion directly influences material deformation, reinforcing the principle that concrete slabs expand proportionally with temperature increments. This observation corresponds with the findings of Assogba et al. (2020), who highlighted that thermal gradients have a linear effect on strain development in rigid pavement structures under seasonal loading conditions.

In the mid-range strain values, such as observations between 0.00328 and 0.00420, a gradual but consistent rise is recorded across all temperature stages. The values start from moderate levels at 25°C and increase smoothly to higher levels at 40°C, without any irregular fluctuations. This suggests that the structural model maintained a stable response to thermal loading in these regions, with deformation occurring predictably as the temperature increased. A similar trend was reported by Smit (2020), who observed that rigid pavements under controlled thermal cycles exhibited consistent strain increments, particularly in centrally supported slab zones, indicating uniform material behaviour.

The lower observations, ranging from 0.00240 to 0.00312, also demonstrate a steady increase, albeit at smaller magnitudes compared to higher strain zones. Despite their relatively lower values, these results show that all regions of the slab, regardless of initial strain levels, respond to thermal influence by expanding progressively. This highlights that temperature loading exerts a universal effect on the structural system, even in sections with less stress concentration. This behaviour agrees with the study of Raffaniello et al. (2022), who found that thermal strain in rigid pavements occurs consistently across the slab, though the magnitudes may vary depending on thickness and material stiffness.

The smallest values, observed in the final group, rise from as low as 0.00065 at 25°C to 0.00108 at 40°C. Although these deflections are minimal, the upward trend confirms that no part of the slab is entirely unaffected by thermal expansion. Even the least responsive regions continue to undergo measurable deformation, pointing to the cumulative impact of temperature on rigid pavement performance. This outcome supports the findings of Zeiada et al. (2023), who emphasized that low-strain zones in pavement structures can still accumulate thermal effects over time, which may contribute to long-term fatigue if not accounted for in design.

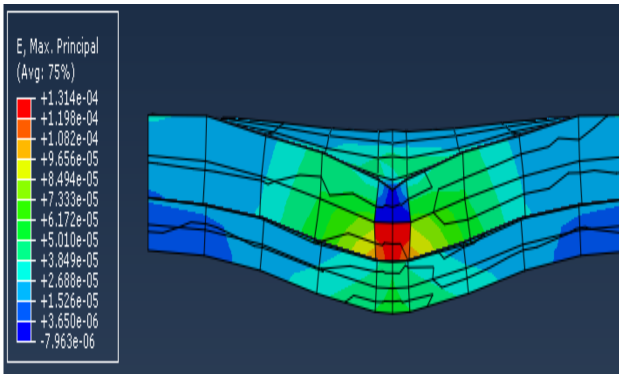

Figure 9: Strain Magnitude of the Structural Model at 25 °C

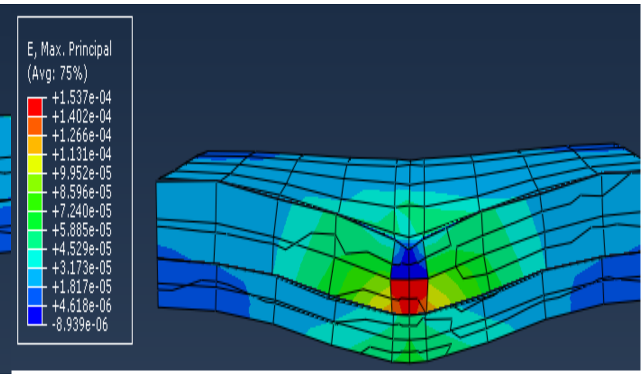

Figure 10: Strain Magnitude of the Structural Model at 30 °C

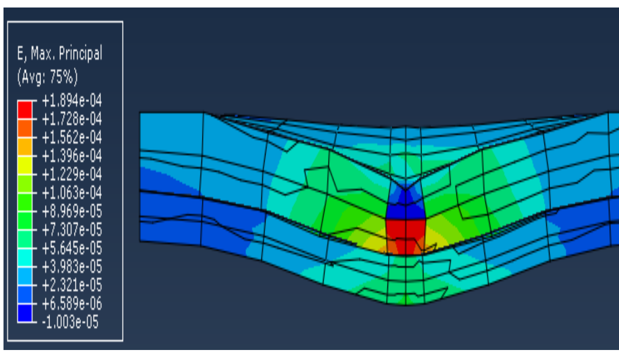

Figure 11: Strain Magnitude of the Structural Model at 35 °C

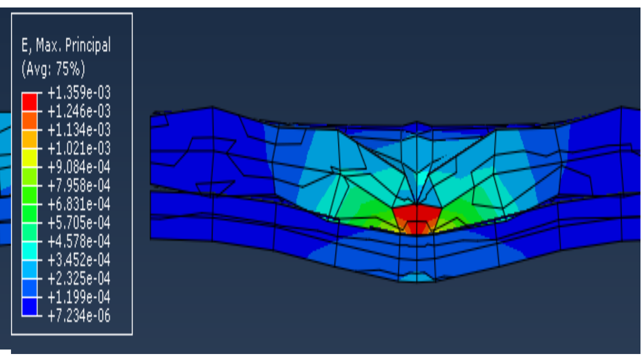

Figure 12: Strain Magnitude of the Structural Model at 40 °C

Performance Evaluation Metrics

The relationships between pavement performance indicators—deflection, strain, and stress—across the evaluated temperature ranges are exceptionally strong and statistically significant. Indeed, the correlation coefficients are consistently above 0.97, which signifies near-perfect associations among the variables as the temperature increases from 25 °C to 40 °C. In particular, deflection at 25 °C exhibits very high correlations with subsequent deflections at 30 °C, 35 °C, and 40 °C, as well as with strain and stress across the same temperature spectrum. Therefore, it can be inferred that thermal variations exert a uniform influence on the mechanical responses of pavement structures, leading to a stable and predictable pattern of deformation and stress distribution.

Furthermore, the relationship between strain and stress across the temperature levels is especially noteworthy, as the correlation coefficients approach unity. This near-perfect association indicates that increases in strain are directly mirrored by proportional increases in stress, irrespective of the thermal load applied. Thus, these results highlight the intrinsic dependency between strain and stress under thermal effects. A similar observation was reported by Sun et al. (2022), who confirmed that thermal gradients in pavement systems generate strong linear associations between induced strain and corresponding stress responses, thereby emphasizing that both indicators are tightly coupled in reflecting material behavior under varying temperatures.

In addition, the consistency of correlations between deflection and both strain and stress across different temperature conditions demonstrates that pavement deflection can reliably serve as a predictor of overall structural response under thermal loading. Notably, the correlations of deflection at 40 °C with strain and stress at the same temperature level are almost absolute, implying that vertical deformation is highly indicative of internal stresses and strains. This finding corresponds with the results of Shen et al. (2025), who emphasized that deflection-based measurements can be effectively employed to infer pavement performance indicators, particularly under environmental stressors such as temperature fluctuations.

Moreover, the statistical significance of all reported correlations, with p-values less than 0.01, further strengthens the validity and reliability of these associations as presented in Table 4.6. Since the correlations remain consistently strong across all temperature levels, it may be concluded that the pavement system exhibits a stable and resilient response mechanism to thermal loading, without major deviations as temperature increases. This observation is consistent with the findings of Huang et al. (2022), who demonstrated that pavements subjected to repeated thermal cycles maintain stable structural interactions among performance metrics, thus reflecting the robustness of well-designed pavement systems against temperature-induced stresses.

Table 7: Pearson Correlations between Pavement Performance Indicators across Temperatures.

Temperature	Variable Pair	r (95% CI)	N	p-value
T1	Deflection–Strain	0.98 (0.94–0.99)	13	<0.001
T1	Deflection–Stress	0.98 (0.93–0.99)	13	<0.001
T2	Deflection–Strain	1.00 (0.99–1.00)	13	<0.001
T2	Deflection–Stress	1.00 (0.99–1.00)	13	<0.001
T3	Deflection–Strain	1.00 (0.99–1.00)	13	<0.001
T3	Deflection–Stress	1.00 (0.99–1.00)	13	<0.001
T4	Deflection–Strain	1.00 (0.99–1.00)	13	<0.001
T4	Deflection–Stress	1.00 (0.99–1.00)	13	<0.001
T1	Strain–Stress	0.99 (0.95–0.99)	13	<0.001
T2	Strain–Stress	0.99 (0.96–1.00)	13	<0.001
T3	Strain–Stress	1.00 (0.99–1.00)	13	<0.001
T4	Strain–Stress	1.00 (0.99–1.00)	13	<0.001

Table 8: Descriptive Statistics of Pavement Performance Indicators across Temperature Levels (T1–T4).

Pavement Indicators	Minimum	Maximum	Mean	Std. Error	Std. Deviation	Variance	Skewness	Kurtosis
Def_T1	0.0514	0.5570	0.299923	0.0446341	0.1609306	0.026	0.095	-1.006
Def_T2	0.1083	0.6210	0.378169	0.0458682	0.1653801	0.027	-0.119	-1.130
Def_T3	0.1465	0.6742	0.424138	0.0473408	0.1706896	0.029	-0.093	-1.171
Def_T4	0.1841	0.7310	0.479985	0.0488218	0.1760295	0.031	-0.170	-1.118
Strain_T1	0.00065	0.00411	0.0025954	0.00032198	0.00116092	0.000	-0.281	-1.215
Strain_T2	0.00074	0.00453	0.0028054	0.00034595	0.00124733	0.000	-0.212	-1.200
Strain_T3	0.00089	0.00493	0.0030885	0.00036679	0.00132247	0.000	-0.221	-1.160
Strain_T4	0.00108	0.00532	0.0033908	0.00038358	0.00138301	0.000	-0.228	-1.162
Stress_T1	284	3280	1890.85	278.025	1002.434	1004873.141	-0.153	-1.348

Stress_T2	211	3487	1909.23	297.577	1072.928	11511 73.526	-0.109	-1.216
Stress_T3	272	3720	2056.46	314.740	1134.812	12877 97.936	-0.073	-1.254
Stress_T4	348	3951	2226.23	326.483	1177.150	13856 83.192	-0.072	-1.227
Valid N (listwise)								

Conclusion

This study revealed that elevated temperatures reduce the thermal and mechanical properties of rigid pavements while increasing deflection, stress, and strain, with correlations above 0.97 confirming the predictable interdependence of these responses. Deflection emerged as a reliable predictor of internal stress–strain behavior under thermal loading. To mitigate heat-induced deterioration, supplementary cementitious materials and climate-responsive design features such as reflective coatings, expansion joints, and efficient load transfer systems are recommended. Real-time deflection monitoring is further proposed as a predictive tool for proactive maintenance and extended service life.

Acknowledgement

I express my deepest gratitude to Almighty God for strength and wisdom throughout this work. Sincere appreciation goes to my supervisor, Dr. O. P. Akintunde, for his invaluable guidance, and to Professor G. M. Ayininuola, Head of the Department of Civil Engineering, University of Ibadan, for his support. I also acknowledge the assistance of the departmental laboratory staff, as well as the encouragement of colleagues, friends, and family whose contributions made this study possible.

References

AASHTO (2020). *Standard Specifications for Transportation Materials and Methods of Sampling and Testing*. 40th Edition, American Association of State Highway and Transportation Officials, Washington, D.C.

Al-Atroush, M. E. (2022). Structural behavior of the geothermo-electrical asphalt pavement: A critical review concerning climate change. *Heliyon*, *8*(12).

Al-Khateeb, G., Alnaqbi, A., and Zeiada, W. (2025). Predictive modeling of punchouts in continuously reinforced concrete pavement: a machine learning approach. *AI in Civil Engineering*, *4*(1), 15.

Al-Qadi, I. L., and Hernandez, J. (2021). *Temperature Responses of Partially Restrained Airfield Rigid Pavement* (No. DOT/FAA/TC-21/31). United States. Department of Transportation. Federal Aviation Administration. William J. Hughes Technical Center.

Alsheyab, M. A., Khasawneh, M. A., Abualia, A., and Sawalha, A. (2024). A critical review of fatigue cracking in asphalt concrete pavement: a challenge to pavement durability. *Innovative infrastructure solutions*, *9*(10), 386.

Assogba, O. C., Tan, Y., Zhou, X., Zhang, C., and Anato, J. N. (2020). Numerical investigation of the mechanical response of semi-rigid base asphalt pavement under traffic load and nonlinear temperature gradient effect. *Construction and Building Materials, 235*, 117406.

ASTM C531-18(2021), *Standard Test Method for Linear Shrinkage and Coefficient of Thermal Expansion of Hydraulic-Cement Mortars and Concretes*, ASTM International, West Conshohocken, PA.

ASTM D5334-22(2021), *Standard Test Method for Determination of Thermal Conductivity of Soil and Soft Rock by Thermal Needle Probe Procedure*, ASTM International, West Conshohocken, PA.

ASTM D7369-11(2021), *Standard Test Method for Determining the Resilient Modulus of Bituminous Mixtures Using Indirect Tension Test*, ASTM International, West Conshohocken, PA.

Bayraktarova, K., Eberhardsteiner, L., Zhou, D., and Blab, R. (2022). Characterisation of the climatic temperature variations in the design of rigid pavements. *International journal of pavement engineering*, *23*(9), 3222-3235.

Benchekkour, A., Terfaya, N., Elmir, M., Kebir, T., and Benguediab, M. (2024). Modeling of delamination process coupling contact, friction, and adhesion considering the thermal effect. *Mater. Phys. Mech*, *51*(3), 146-66.

Cai, P., Chai, Y., Tighe, S., Wang, M., and Yin, S. (2025). Optimization of the Photovoltaic Panel Design Towards Durable Solar Roads. *Inventions*, *10*(4), 70.

Ceylan, H., Gopalakrishnan, K., Kim, S., Taylor, P., Alhasan, A., and Yang, S. (2016). *Impact of curling and warping on concrete pavement* (No. IHRB Project TR-668). Iowa State University. National Concrete Pavement Technology Center.

Gong, F., Jiang, X., Gamil, Y., Iftikhar, B., and Thomas, B. S. (2023). An overview on spalling behavior, mechanism, residual strength and microstructure of fiber reinforced concrete under high temperatures. *Frontiers in Materials*, *10*, 1258195.

Kildashti, K., Katwal, U., Tao, Z., and Tam, V. (2024). Numerical simulation of steel-concrete composite beams and slabs at elevated temperatures. *Engineering Structures*, *315*, 118297.

Li, M., Dai, Q., Su, P., and You, Z. (2024). Buckling prediction based on joint opening and safe temperature estimation in jointed plain concrete pavements. *Construction and Building Materials*, *444*, 137630.

Li, Y., Han, X., Zhang, D., Li, J., Miao, P., and Wang, W. (2025). Temperature–Load Stress Analysis of Ultra-Long Pool Structures Based on Distributed Fiber Optic Sensing and Finite Element Analysis. *Buildings*, *15*(16), 2961.

Liu, Z., Gu, X., Ren, H., Zhou, Z., Wang, X., and Tang, S. (2022). Analysis of the dynamic responses of asphalt pavement based on full-scale accelerated testing and finite element simulation. *Construction and Building Materials*, *325*, 126429.

Llopis-Castelló, D., García-Segura, T., Montalbán-Domingo, L., Sanz-Benlloch, A., and Pellicer, E. (2020). Influence of pavement structure, traffic, and weather on urban flexible pavement deterioration. *Sustainability*, *12*(22), 9717.

Ma, R., Li, Y., Cheng, P., Chen, X., and Cheng, A. (2024). Low-Temperature Cracking and Improvement Methods for Asphalt Pavement in Cold Regions: A Review. *Buildings*, *14*(12), 3802.

Moffatt, M. A. (2015). *Improved consideration of multiple-axle loads in the structural design of flexible pavements* (Doctoral dissertation, Monash University).

Pour, A. K. (2023). *Thermal Behavior of Plain and Fiber-Reinforced Rigid Concrete Airfield Runways* (Doctoral dissertation, The University of Texas at El Paso).

Qiao, Y., Dawson, A. R., Parry, T., Flintsch, G., and Wang, W. (2020). Flexible pavements and climate change: A comprehensive review and implications. *Sustainability*, *12*(3), 1057.

Qin, Y., Zhang, X., Tan, K., and Wang, J. (2022). A review on the influencing factors of pavement surface temperature. *Environmental Science and Pollution Research*, *29*(45), 67659-67674.

Raffaniello, A., Bauer, M., Safiuddin, M., and El-Hakim, M. (2022). Traffic and climate impacts on rutting and thermal cracking in flexible and composite pavements. *Infrastructures*, *7*(8), 100.

Safiuddin, M., Kaish, A. A., Woon, C. O., and Raman, S. N. (2018). Early-age cracking in concrete: Causes, consequences, remedial measures, and recommendations. *Applied Sciences*, *8*(10), 1730.

Shen, K., Wang, H., Canestrari, F., and Graziani, A. (2025). Temperature correction for traffic speed deflectometer measurements on flexible pavement using ANN models. *Road Materials and Pavement Design*, *26*(sup1), 751-770.

Smarzewski, P. (2019). Study of toughness and macro/micro-crack development of fibre-reinforced ultra-high performance concrete after exposure to elevated temperature. *Materials*, *12*(8), 1210.

Smit, M. S. (2020). *Response of ultra-thin continuously reinforced concrete pavement to traffic loading* (Doctoral dissertation, University of Pretoria (South Africa)).

Subedi, A., Kim, H., Lee, M. S., and Lee, S. J. (2025). Thermal Behavior of Concrete: Understanding the Influence of Coefficient of Thermal Expansion of Concrete on Rigid Pavements. *Applied Sciences (2076-3417)*, *15*(6).

Sun, Y., Zhang, Z., Gong, H., Zhou, C., Chen, J., and Huang, B. (2022). 3D multiscale modeling of asphalt pavement responses under coupled temperature–stress fields. *Journal of Engineering Mechanics*, *148*(3), 04022010.

Wu, H., Sun, B., Li, Z., and Yu, J. (2018). Characterizing thermal behaviors of various pavement materials and their thermal impacts on ambient environment. *Journal of cleaner production*, *172*, 1358-1367.

Wu, Z., and Mahdi, M. I. (2022). *Application of Mechanistic-Empirical Pavement Design Approach Into RCC Pavement Thickness Design* (No. FHWA/LA. 22/671). Louisiana Transportation Research Center.

Yang, Y., Miao, L., and Chow, C. L. (2018). Relative significance of temperature gradient components on cracking behavior in glass panes under thermal radiation. *Applied Thermal Engineering*, *131*, 837-848.

Yannis, G., and Chaziris, A. (2022). Transport system and infrastructure. *Transportation research procedia*, *60*, 6-11.

Zeiada, W., Abu Dabous, S., Al-Ruzouq, R., Hamad, K., Souliman, M. I., and Mirou, S. (2023). Effect of air voids and asphalt content changes on laboratory and simulated long-term fatigue performance of asphalt concrete pavements. *Innovative Infrastructure Solutions*, *8*(1), 48.